MATCH
Communications in Mathematical and in Computer Chemistry

MATCH Commun. Math. Comput. Chem. **82** (2019) 181-201

ISSN 0340 - 6253

The Saturation Number of Carbon Nanocones and Nanotubes

Taylor Short*

Department of Mathematics
Grand Valley State University
shorttay@gvsu.edu

(Received July 30, 2018)

Abstract

The saturation number of a graph is the cardinality of a smallest maximal matching. This paper presents bounds for the saturation number of carbon nanocones which are asymptotically equal. The same techniques are applied for the saturation number of a certain family of carbon nanotubes, which improve previous results and in one case, yields the exact value.

1 Introduction

Throughout this paper G is an n-vertex, simple graph with vertex set $V(G)$ and edge set $E(G)$. A *matching* M in a graph G is a collection of edges of G such that no two edges from M share a vertex. The cardinality of M is called the *size* of the matching. A matching M is a *maximum matching* if there is no matching in G with greater size. The *matching number*, $\nu(G)$, of G is the cardinality of any maximum matching in G. Since each vertex can be incident to at most one edge of a matching, it follows that $\nu(G) \leq \lfloor n/2 \rfloor$ for any graph G. If every vertex of G is incident with an edge in M, then M is called a *perfect* matching and such graphs have $\nu(G) = n/2$. It is clear that perfect matchings are also maximum matchings but the converse is not generally true.

*This work was partially supported by a SPARC Graduate Research Grant from the Office of the Vice President for Research at the University of South Carolina.

Matchings serve as models of many phenomena across the sciences. An important motivation for their study arose from chemistry, when it was observed that the stability of benzenoid compounds is related to the number of perfect matchings, also known as *Kekulé structures*, in the corresponding chemical graphs. For a survey of these results, see [7]. With the discovery of fullerenes in 1985 [22], the desire to identify properties characteristic for stable fullerenes led to the enumeration of perfect matchings [8,9,19,26] in these corresponding graphs.

Maximum matchings give one way to quantify the largeness of a matching. Both the enumerative and structural properties of maximum matchings are well studied and well understood, see [23] for a general background on such matching theory.

There is yet another way to quantify the largeness of a matching. A *maximal matching* in G is a matching that cannot be extended to a larger matching in G. Clearly, every maximum matching is also maximal but the opposite is usually not true. Chemically, maximal matchings model the adsorption of dimers to a molecule, where each dimer bonds to a pair of adjacent atoms in the molecule. Any such adsorption pattern corresponds to a matching in the graph of the molecule, and once no further adsorption is possible, such a matching must be maximal. The best case of adsorption can be viewed as a maximum matching, while the worst case concerns the smallest possible maximal matching. This idea gives rise to the study of the *saturation number* of a graph G, which is the cardinality of any smallest maximal matching in G. Thus the saturation number is a measure of how inefficient the adsorption process can be. Aside from chemistry, the saturation number has a number of interesting applications in networks, engineering, etc. The saturation number of a graph is equal to the cardinality of a minimum independent edge dominating set. Finding an independent edge dominating set in a graph is an NP-Hard problem [25].

Maximal matchings are much less understood than their maximum counterparts. Some work has been done on enumerating maximal matchings in certain chemical graphs [11, 14] but this area remains largely unexplored. Structural properties, such as the saturation number, have been studied for benzenoid graphs [12, 13], fullerenes [2, 3, 10], and nanotubes [24]. The paper [13] mentions the saturation number of nanocones as an interesting, unexplored avenue of study.

This paper considers both nanocones and nanotubes, which are carbon networks situated between graphene and fullerene in terms of structure. New upper and lower bounds on the saturation number of nanocones are established, which are asymptotically equal. In addition, lower bounds for the saturation number of two classes of nanotubes are presented, which improve recent results [24].

2 Statement of Results

Let G be connected, bridgeless plane graph such that all vertices have degree 2 or 3. A face of G whose boundary is a cycle of length 6 is called a *hexagon* and any other face bounded by a cycle of length $k \geq 3$ and $k \neq 6$ is called a *k-defect* or just *defect* when there is no need to specify the cycle length. Moreover, a defect is called *internal* if all vertices incident to the face are degree 3. A defect E is *external* if there are degree 2 vertices incident to the face and let $n_2(E)$ be the number of degree 2 vertices incident to E. If the outer face of G is an external defect and if all the external defects are pairwise disjoint (they have no vertex in common) then G is called a *patch*.

Next it will be useful to introduce some definitions utilized in [4, 5, 15–17]. A *break edge* is an edge incident to an external defect whose endpoints are both degree 2. A *bend edge* is an edge incident to an external defect whose endpoints are both degree 3. A patch is *pseudoconvex* if it does not contain any bend edges. A *side* of a patch is a path along the outer face between a consecutive pair of break edges, including the break edges, and the *length* of a side is the number of degree 3 vertices on the side.

The following theorem is the main tool in proving lower bounds on the saturation number. This theorem is an extension of the theorem proven for fullerenes in [3]. For the sake of consistency, the proof in Section 3 uses similar terminology and structure to what was presented in [3].

Theorem 2.1. *Let G be a pseudoconvex patch with n vertices, o_k internal k-defects where k is odd, e_k k-defects where $k \neq 6$ is even, and n_2 vertices of degree 2. Then*

$$s(G) \geq \frac{n}{3} - \frac{1}{18}\left(\sum_{k\ odd}(k-2)o_k + \sum_{k\ even} ke_k\right) - \frac{n_2}{6}.$$

2.1 Nanocones

Generally speaking, nanocones are planar graphs where the majority of faces are hexagons, along with some non-hexagonal faces, most commonly pentagons, in addition to the outer face. This paper considers these pentagonal defect nanocones as well as nanocones with a single defect.

A *single-defect k-gonal nanocone with ℓ layers*, $CNC_k(\ell)$, is obtained by taking a cycle on $k \geq 3$ vertices, C_k, and surrounding it with ℓ concentric layers of hexagons. Using previous terminology, a single-defect k-gonal nanocone is a pseudoconvex patch with a single k-defect at its apex. By induction, it follows that there are $k\binom{\ell+1}{2}$ hexagonal faces, $k(\ell+1)^2$ total vertices, and $(2\ell+1)k$ external vertices. There are $k\ell$ external vertices of degree 3 and $k(\ell+1)$ vertices of degree 2. The following Corollary is an immediate consequence of Theorem 2.1.

Corollary 2.2.

$$s(CNC_k(\ell)) \geq \begin{cases} \frac{k(\ell+1)^2}{3} - \frac{k-2}{18} - \frac{k(\ell+1)}{6} & \text{if } k \text{ is odd} \\ \frac{k(\ell+1)^2}{3} - \frac{k}{18} - \frac{k(\ell+1)}{6} & \text{if } k \text{ is even} \end{cases}$$

Pentagonal defect nanocones are pseudoconvex patches with p internal 5-defects (or pentagons), where $1 \leq p \leq 5$, and no other internal defects. While many arrangements of pentagons and hexagons are possible, a classification result first from [20, 21] and then independently in [18] shows that it suffices to consider the 8 configurations of pentagons and or hexagons in Figure 1. Note that the single pentagon configuration is merely $CNC_5(0)$.

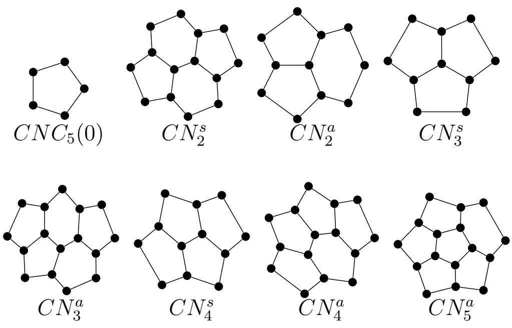

Figure 1. The 8 configurations of pentagons and or hexagons for pentagonal defect nanocones.

A *pentagonal defect nanocone with i pentagons and ℓ layers*, $CN_i^j(\ell)$, $i \in \{2,3,4,5\}$ and $j \in \{s,a\}$, is defined to be the configuration CN_i^j in Figure 1 surrounded by ℓ concentric layers of hexagons. For reference, the use of s in the superscript designates a symmetric configuration as drawn in Figure 1 and the use of a represents asymmetric. The configurations $CNC_5(0)$ and CN_i^j in Figure 1 are called the *caps* of the nanocone.

The following Corollary is another consequence of Theorem 2.1, and its proof, containing additional details, is provided in Section 4.

Corollary 2.3. *(a)* $s(CN_2^s(\ell)) \geq \frac{14+4\ell(\ell+4)}{3} - \frac{1}{3} - \frac{4(\ell+2)}{6}$

(b) $s(CN_2^a(\ell)) \geq \frac{11+2\ell(2\ell+7)}{3} - \frac{1}{3} - \frac{4\ell+7}{6}$

(c) $s(CN_3^s(\ell)) \geq \frac{10+3\ell(\ell+4)}{3} - \frac{1}{2} - \frac{3(\ell+2)}{6}$

(d) $s(CN_3^a(\ell)) \geq \frac{16+\ell(3\ell+16)}{3} - \frac{1}{2} - \frac{3\ell+8}{6}$

(e) $s(CN_4^s(\ell)) \geq \frac{12+2\ell(\ell+6)}{3} - \frac{2}{3} - \frac{2(\ell+3)}{6}$

(f) $s(CN_4^a(\ell)) \geq \frac{15+2\ell(\ell+7)}{3} - \frac{2}{3} - \frac{2\ell+7}{6}$

(g) $s(CN_5^a(\ell)) \geq \frac{16+\ell(\ell+12)}{3} - \frac{5}{6} - \frac{\ell+6}{6}$

The upper bound on the saturation number of nanocones relies on splitting the nanocone in subgraphs, where the number of subgraphs depends on the number of break edges. The following Lemma was proven in [17].

Lemma 2.4. *[17] In a pentagonal defect nanocone, the number of pentagons p and the number of break edges s are related by*

$$s + p = 6.$$

The subgraph used is a *benzenoid triangle*, T_p, which is a patch that can be constructed by arranging $\binom{p+1}{2}$ hexagonal faces in the shape of an equilateral triangle, so that each side of the triangle has p hexagons. For an example of a benzenoid triangle see Figure 2. Note that the saturation number of similar graphs, such as benzenoid parallelograms, was studied in [13]. The upper bound on the saturation number of benzenoid triangles is presented in Lemma 2.5 which is used to deduce the upper bounds on the saturation number of nanocones in Theorem 2.6. The proofs of these results are presented in Section 4.

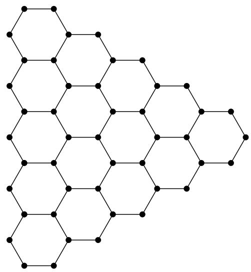

Figure 2. The benzenoid triangle, T_5.

Lemma 2.5.

$$s(T_p) \leq \left\lfloor \frac{(p+1)(p+3)}{3} \right\rfloor$$

The upper bound presented in Lemma 2.5 is believed to be the exact value of $s(T_p)$ and is the sequence A032765 in the OEIS [1].

Theorem 2.6. *(a)* $s(CNC_k(\ell)) \leq k \left\lfloor \frac{\ell(\ell+2)}{3} \right\rfloor + k(\ell+1)$

(b) $s(CN_2^s(\ell)) \leq 4 \left\lfloor \frac{(\ell+1)(\ell+3)}{3} \right\rfloor + 4(\ell+1) + 1$

(c) $s(CN_2^a(\ell)) \leq 3 \left\lfloor \frac{(\ell+1)(\ell+3)}{3} \right\rfloor + \left\lfloor \frac{\ell(\ell+2)}{3} \right\rfloor + 4(\ell+1) + 1$

(d) $s(CN_3^s(\ell)) \leq 3 \left\lfloor \frac{(\ell+1)(\ell+3)}{3} \right\rfloor + 3(\ell+1) + 1$

(e) $s(CN_3^a(\ell)) \leq 2 \left\lfloor \frac{(\ell+2)(\ell+4)}{3} \right\rfloor + \left\lfloor \frac{(\ell+1)(\ell+3)}{3} \right\rfloor + 3(\ell+1) + 2$

(f) $s(CN_4^s(\ell)) \leq 2 \left\lfloor \frac{(\ell+2)(\ell+4)}{3} \right\rfloor + 2(\ell+1) + 3$

(g) $s(CN_4^a(\ell)) \leq \left\lfloor \frac{(\ell+3)(\ell+5)}{3} \right\rfloor + \left\lfloor \frac{(\ell+2)(\ell+4)}{3} \right\rfloor + 2(\ell+1) + 4$

(h) $s(CN_5^a(\ell)) \leq \left\lfloor \frac{(\ell+5)(\ell+7)}{3} \right\rfloor + (\ell+1) + 6$

Combining Corollaries 2.2 and 2.3 along with Theorem 2.6 shows that if G is any nanocone graph with n vertices, then $s(G)$ is asymptotically equal to $n/3$. Hence, in a smallest maximal matching, as n gets large there are roughly 2 matched edges per hexagon. These findings are consistent with the work done on the saturation number of fullerenes [3] and benzenoid graphs [13].

2.2 Nanotubes

Open ended nanotubes, also called *tubulenes*, can be obtained in the following way. Starting with a hexagonal tessellation of a cylinder, take the finite graph induced by all hexagons that lie between two vertex disjoint cycles, where each cycle encircles the axis of the cylinder. This paper considers two types of tubulenes having particularly nice structure, namely zig-zag and armchair tubulenes, shown in Figures 3 and 4.

Zig-zag tubulenes, $ZT(\ell, m)$, have ℓ horizontal layers of hexagons, each containing m hexagons. Bounds on the saturation number of such zig-zag were first established in [24], shown in Corollary 2.7.

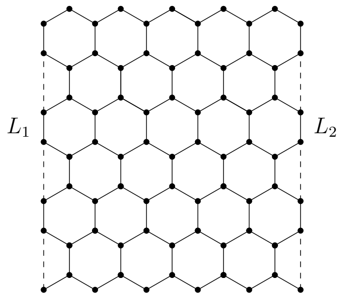

Figure 3. The zig-zag tubulene, $ZT(6,5)$, is obtained from the figure above by gluing the lines L_1 and L_2 together.

Corollary 2.7. *[24]*

$$\frac{m(\ell+1)}{2} \leq s(ZT(\ell,m)) \leq \begin{cases} \frac{m(2\ell+3)}{3} & \textit{if } 3|\ell \\ \frac{m(2\ell+1)}{3} & \textit{if } 3|(\ell-1) \\ \frac{m(2\ell+2)}{3} & \textit{if } 3|(\ell-2) \end{cases}$$

Corollary 2.8 follows as an application of Theorem 2.1 and improves the lower bound for the saturation number of zig-zag tubulenes. The proof is contained in Section 5.

Corollary 2.8.

$$s(ZT(\ell,m)) \geq \frac{m(2\ell+1)}{3}$$

Combining the new lower bound from Corollary 2.8 and the upper bounds presented in Corollary 2.7, it follows that $s(ZT(\ell,m)) = \frac{m(2\ell+1)}{3}$ whenever $3|(\ell-1)$.

It follows that the saturation number of zig-zag tubulenes with n vertices is asymptotically equal to $n/3$. This is now consistent with the findings for nanocones, fullerenes, and benzenoid graphs.

Armchair tubulenes, $AT(m, \ell)$, have ℓ vertical layers of hexagons, each containing m hexagons. The saturation number of armchair tubulenes was also studied in [24], as seen in Corollary 2.9.

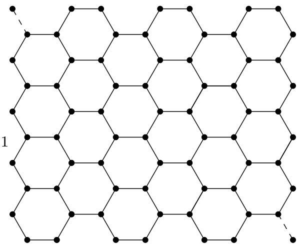

Figure 4. The armchair tubulene, $AT(4, 6)$, is obtained from the figure above by gluing the curves L_1 and L_2 together.

Corollary 2.9. *[24]*

$$\frac{\ell(m+1)}{2} \leq s(AT(m,\ell)) \leq \begin{cases} \frac{2\ell(m+1)}{3} & \textit{if } 3|\ell \\ \frac{(2\ell+1)(m+1)}{3} & \textit{if } 3|(\ell-1) \\ \frac{2(\ell+2)(m+1)}{3} & \textit{if } 3|(\ell-2) \end{cases}$$

However, while armchair tubulenes are patches, they are not pseudoconvex, so Theorem 2.1 does not apply. Closing the gap on the saturation number of armchair tubulenes remains an open problem.

3 Proof of the main tool

Proof (of Theorem 2.1). Let M be a maximal matching in G. Let the edges in M and the vertices saturated by M be called black, and let the remaining edges and vertices be called white. Let B and W be the set of all black and white vertices, respectively.

The proof using the discharging method, setting the initial charges as follows:

- Let the initial charge of each black vertex be 3;
- Let the initial charge of each white vertex be -6;

- Let the initial charge of each k-defect be equal to $\begin{cases} k-2 & \text{if } k \text{ is odd,} \\ k & \text{if } k \text{ is even} \end{cases}$; and
- Let the initial charge of each external defect, E, be $3n_2(E)$.

It remains to show that the total sum of the charge in the graph $3|B| - 6|W| + \sum_{k \text{ odd}}(k-2)o_k + \sum_{k \text{ even}} ke_k + 3n_2$ is non-negative. From this it follows that

$$3|B| \geq 2|B| + 2|W| - \frac{1}{3}\left(\sum_{k \text{ odd}}(k-2)o_k + \sum_{k \text{ even}} ke_k\right) - n_2$$

implying that

$$\begin{aligned} |M| = \frac{|B|}{2} &\geq \frac{|B|+|W|}{3} - \frac{1}{18}\left(\sum_{k \text{ odd}}(k-2)o_k + \sum_{k \text{ even}} ke_k\right) - \frac{n_2}{6} \\ &= \frac{n}{3} - \frac{1}{18}\left(\sum_{k \text{ odd}}(k-2)o_k + \sum_{k \text{ even}} ke_k\right) - \frac{n_2}{6}. \end{aligned}$$

The initial charge is distributed as follows:

(R1) Each external defect sends +3 charge to each incident, degree 2 white vertex.

First note that all vertices of degree 2 in G are incident to an external defect, and since the external defects are pairwise disjoint, no vertex of degree 2 is incident to more than one external defect. There are a total of $n_2(E)$ vertices of degree 2 incident to an external defect E, not all of them white vertices, so after applying (R1) all white vertices of degree 2 in G now have charge -3.

(R2) Each white vertex distributes its negative charge evenly among the adjacent black vertices.

Since M is a maximal matching, W is an independent set in G, so no 2 white vertices are adjacent. The white vertices of degree 2 are adjacent to exactly 2 black vertices and sends -1.5 charge to each adjacent black vertex. All other white vertices are adjacent to 3 black vertices and sends -2 charge to each adjacent black vertex. After applying (R2), all white vertices have charge 0.

Let v be a black vertex. Since v is saturated by M, v is adjacent to at least one black vertex and hence, v is adjacent to at most 2 white vertices. After receiving charge 0, -1.5, -2, -3, -3.5, or -4 from (R2) according to the number and type of white neighbors, v now has charge 3, 1.5, 1, 0, -0.5, or -1.

Next, let e_v be the black edge incident with v, and let f_v be the face incident to v but not e_v, if such a face exists. Note that it's possible f_v is an external defect. If such a face does not exists, then both v and e_v must be incident to an external defect, in which case set u_v to be the incident external defect.

(R3) Each black vertex sends all of its remaining charge to f_v or u_v.

Note that all charge that was initially present at the vertices of G is now at its faces. Due to the fact that G is pseudoconvex, it is straightforward to check that if v is a black vertex that sent charge to an external defect according to (R3), then v previously had charge 0, 1, 1.5, or 3. So external defects receive no negative charge after applying (R3), and hence, their total charge is non-negative.

Now the only case when a face receives negative charge from (R3) is when a black vertex v with 2 white neighbors sends charge -1 or $-\frac{1}{2}$ (depending on the degrees of the white neighbors) to f_v. So if a face is incident with at most 1 white vertex, then its charge is certainly non-negative. It turns out that if a face is incident to at most two white vertices, then its charge is non-negative.

An internal k-defect is incident to at most $k/2$ white vertices if k is even and $(k-1)/2$ white vertices if k is odd. Hence, the negative charge an internal k-defect receives after applying (R3) is at most $k/2$ in either case. Therefore, the charge of each such defect is at least $\lfloor k/2 \rfloor$ after applying (R3). Let internal defects be called *good* faces.

All hexagonal faces have nonnegative charge except those incident to three white vertices. For the hexagons incident to at least two white vertices, the different cases for hexagons are split into figures depending on the number of incident vertices of degree 2. The cases for hexagons incident to 0, 1, 2, and 3 vertices of degree 2 can be seen in Figures 5, 6, 7, and 8, respectively. Note that a hexagon incident to 4 vertices of degree 2 receives no negative charge, since any incident black vertex has nonnegative charge after applying (R2). Hexagons cannot be incident to ore than 4 vertices of degree 2, unless the patch consists of a single hexagon, as patches are both bridgeless and connected.

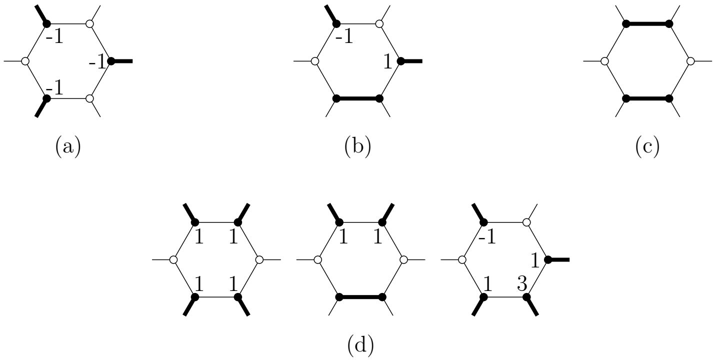

Figure 5. Hexagons adjacent to at least 2 white vertices and 0 vertices of degree 2.

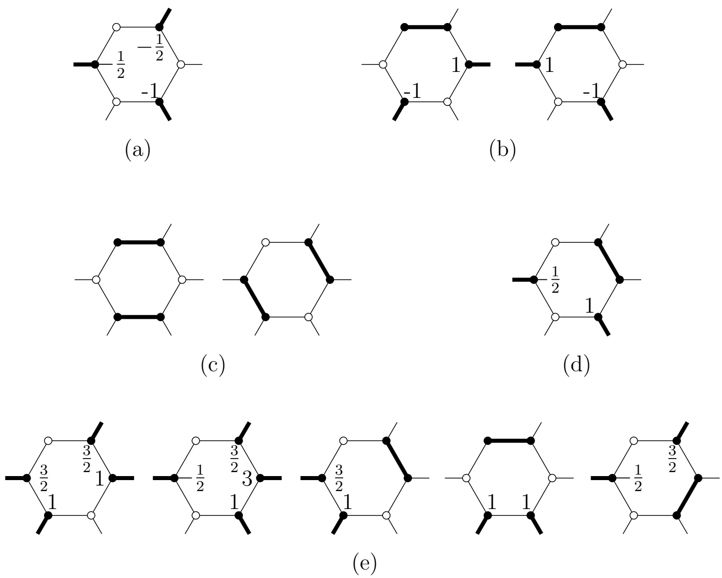

Figure 6. Hexagons adjacent to at least 2 white vertices and 1 vertex of degree 2.

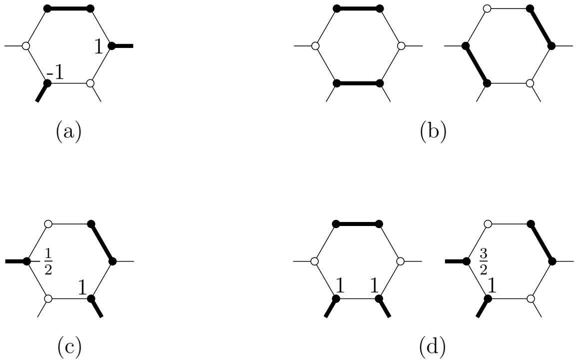

Figure 7. Hexagons adjacent to at least 2 white vertices and 2 vertices of degree 2.

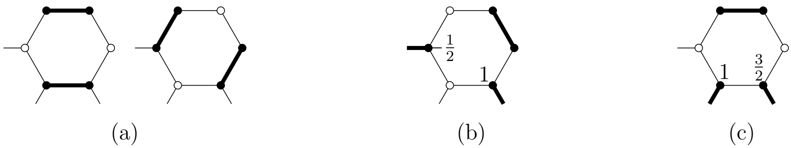

Figure 8. Hexagons adjacent to at least 2 white vertices and 3 vertices of degree 2.

If a hexagon has negative charge as in Figure 5 (a) or Figure 6 (a), then these hexagons are called *bad*. If a hexagon has zero charge as in Figure 5 (b), Figure 6 (b), or Figure 7 (a), then these hexagons are called *transitional*. If a hexagon has zero charge as in Figure 5 (c), Figure 6 (c), Figure 7 (b), or Figure 8 (a), then these hexagons are called *neutral*. Those hexagons with charge 1/2 as in Figure 6 (d), Figure 7 (c), or Figure 8 (b) are called *almost neutral*. All other hexagons have a positive charge, and the value of the positive charge is at least the number of incident white vertices of degree 3; let these hexagons also be called *good* in addition to the internal defects.

Let f be a transitional hexagon. Then f is incident to one black edge, two white vertices, and two black vertices that are incident to black edges not incident to f. Let the white vertex adjacent to the black edge incident to f be called *outgoing*. Let the other white vertex, between the black edges that are not incident to f, be called *incoming*.

The last steps of the discharging are given by the following rules:

(R4) Each good face sends charge 1 to each incident, degree 3 white vertex.

(R5) Each bad hexagon sends charge -1 to each incident, degree 3 white vertex.

(R6) Each transitional hexagon sends charge -1 to the incoming degree 3 white vertex, and it sends charge 1 to the outoing degree 3 white vertex.

After applying (R4)-(R6), there is no negative charge left at the faces of G, and the only possible negative charge resides at white vertices of degree 3 in G.

Let v be a vertex that was sent charge -1 by either (R5) or (R6), let h be the hexagon that sent the negative charge to v, and let u_i, $i = 1, 2$, be the black vertices adjacent to v and incident to h. Since h is either a bad hexagon or transitional hexagon, then the black edges incident to the u_i are not incident to h, see Figure 9.

Now let x be the black vertex adjacent to v but not incident to h. Since G is pseudoconvex, there exists two faces f_i, $= 1, 2$, incident with v different from h, where f_i is incident to u_i, $i = 1, 2$. Without loss of generality, assume the black edge incident with x is incident with f_1. Since the black edges incident to both u_1 and x are incident to f_1, it follows that f_1 is either good or neutral, so it does not send negative charge to v.

Now consider f_2. Since the black edge incident to u_2 is incident to f_2, then f_2 cannot be a bad hexagon, nor a neutral hexagon due to the black edge incident to x. Furthermore, f_2 cannot be almost-neutral since v is a degree 3 white vertex. If f_2 is not incident to any other white vertex other than v, then f_2 is a good hexagon. If f_2 is incident to another white vertex at distance 3 from v, then it is a good hexagon as well. If f_2 is incident to another white vertex at distance 2 from v, then f_2 is a transitional hexagon. In the case that f_2 is transitional, then v is the outgoing white vertex for f_2. Hence in all considered cases, f_2 has sent positive 1 charge to v by (R4) or (R6).

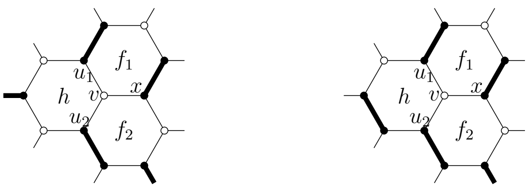

Figure 9. On the left shows the case when h is a bad hexagon and f_2 is transitional. On the right shows when both h and f_2 are transitional.

Thus after these last steps of discharging, there is no negative charge in the graph. So the total sum of charge is non-negative, which finishes the proof. ■

Remark: Repeating the concluding argument to the proof of Theorem 2.1, it's possible G has a chain of adjacent, transitional hexagons, which in turn, would move charge between adjacent hexagons. If such a chain starts with a bad hexagon, then the chain cannot close on itself forming a cycle of hexagons. Such a cycle would have to close at the bad hexagon, implying a white vertex receives negative charge from both a bad hexagon and transitional hexagon and this cannot happen according to the above argument. A chain beginning with a transitional hexagon could close to form a cycle of transitional hexagons, in which case, since transitional hexagons have zero charge, the discharging simply moved zero charge around in a cycle.

4 Proofs for nanocones

Proof (of Lemma 2.5). First a construction of a maximal matching M is given and then below it is shown this matching yields the desired bound. To construct M, T_p is drawn in the plane so that the hexagons appear in columns and the number of hexagons in columns decreases moving to the right, as in Figure 10. Moving left to right, the following pattern of matched edges is iterated every 3 columns of hexagons: the first column of k hexagons requires $k+1$ matched edges, the second column of $k-1$ hexagons requires k matched edges, and the third column is skipped, since edges from the second column partially matches the third column. See the bold edges in Figure 10 for examples of these matchings. This pattern is continued so long as there are at least 3 columns of hexagons remaining, at which point the pattern breaks. This process yields a maximal matching of size

$$(p+1) + p + (p-2) + (p-3) + \cdots + k_2 + k_1$$

where the end values k_i, $i = 1, 2$, fall into 3 cases depending on the value of $p+1$ modulo 3, which can be seen in the matchings of T_3, T_4, and T_5 in Figure 10.

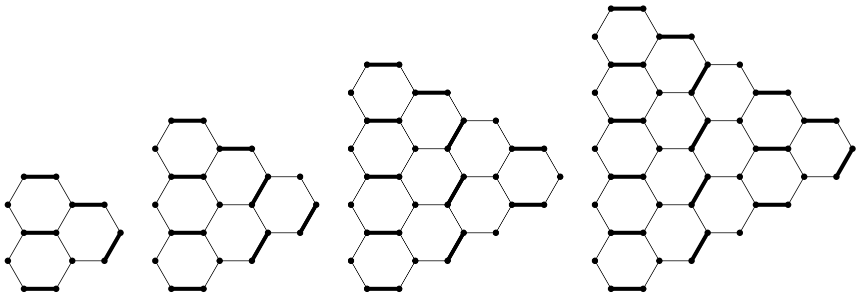

Figure 10. Maximal matchings of T_2, T_3, T_4, and T_5 as described in Lemma 2.5.

The remaining argument is broken into these 3 cases:

(Case 1) $p + 1 \equiv 0 \pmod 3$

In this case, the construction gives a matching of size

$$((p+1)+p)+((p-2)+(p-3))+\cdots+(6+5)+(3+2)$$

and then iteratively rearranging terms so that the next largest term is now paired with the next smallest term yields

$$((p+1)+2)+(p+3)+((p-2)+5)+((p-3)+6)+\cdots((p-k)+(k+3))$$

for some value k. This new sum consists of $(p+1)/3)$ pairs each summing to $(p+3)$, so the matching has size exactly $(p+1)(p+3)/3$.

(Case 2) $p + 1 \equiv 1 \pmod 3$

In this case, it also follows that $(p+3) \equiv 0 \pmod 3$. The construction gives a matching of size

$$((p+1)+p)+((p-2)+(p-3))+\cdots+(4+3)+1$$

which can be rearranged to

$$((p+1)+0)+(p+1)+((p-2)+3)+((p-3)+4)+\cdots((p-k)+(k+1))$$

for some value k. This new sum consists of $(p+3)/3)$ pairs each summing to $(p+1)$, so the matching has size exactly $(p+1)(p+3)/3$.

(Case 3) $p+1 \equiv 2 \pmod 3$

This case has $(p+1) = 3q+2$ for some integer q. The construction gives a matching of size

$$((p+1)+p)+((p-2)+(p-3))+\cdots+(5+4)+2.$$

First, the smallest and largest terms are paired together, $((p+1)+2)$, and the next largest term, p, is reserved. The remaining terms are iteratively rearranged so that the next largest term is now paired with the next smallest term to obtain

$$((p-2)+4)+((p-3)+5)+\cdots((p-k)+(k+2))$$

for some value k. This last sum results in $(q-1)$ pairs each summing to $(p+2)$. Hence the matching has size $(p+3)+p+(q-1)(p+2)$. Now

$$\begin{aligned}
(p+3)+p+(q-1)(p+2) &= (p+3)+p+(q-1)(p+3)-(q-1) \\
&= p+q(p+3)-(q-1) \\
&= p-\frac{p-4}{3}+q(p+3) \\
&< \frac{2}{3}(p+3)+q(p+3) \\
&= \frac{(p+1)(p+3)}{3}
\end{aligned}$$

which proves the desired bound. ■

Proof (of Corollary 2.3). The claimed lower bounds are a straight forward application of Theorem 2.1 depending on the total number of vertices, the number of pentagons, and the number of vertices of degree 2. The counts of these values are provided below, where both counts of vertices follow by induction on ℓ.

(a) $CN_2^s(\ell)$ has $14+4\ell(\ell+4)$ total vertices, 2 pentagons, and $4(\ell+2)$ vertices of degree 2.

(b) $CN_2^a(\ell)$ has $11+2\ell(2\ell+7)$ total vertices, 2 pentagons, and $4\ell+7$ vertices of degree 2.

(c) $CN_3^s(\ell)$ has $10+3\ell(\ell+4)$ total vertices, 3 pentagons, and $3(\ell+2)$ vertices of degree 2.

(d) $CN_3^a(\ell)$ has $16+\ell(3\ell+16)$ total vertices, 3 pentagons, and $3\ell+8$ vertices of degree 2.

(e) $CN_4^s(\ell)$ has $12 + \ell(2\ell + 12)$ total vertices, 4 pentagons, and $2(\ell + 3)$ vertices of degree 2.

(f) $CN_4^a(\ell)$ has $15+\ell(2\ell+14)$ total vertices, 4 pentagons, and $2\ell+7$ vertices of degree 2.

(g) $CN_5^a(\ell)$ has $16+\ell(\ell+12)$ total vertices, 5 pentagons, and $\ell+6$ vertices of degree 2. ■

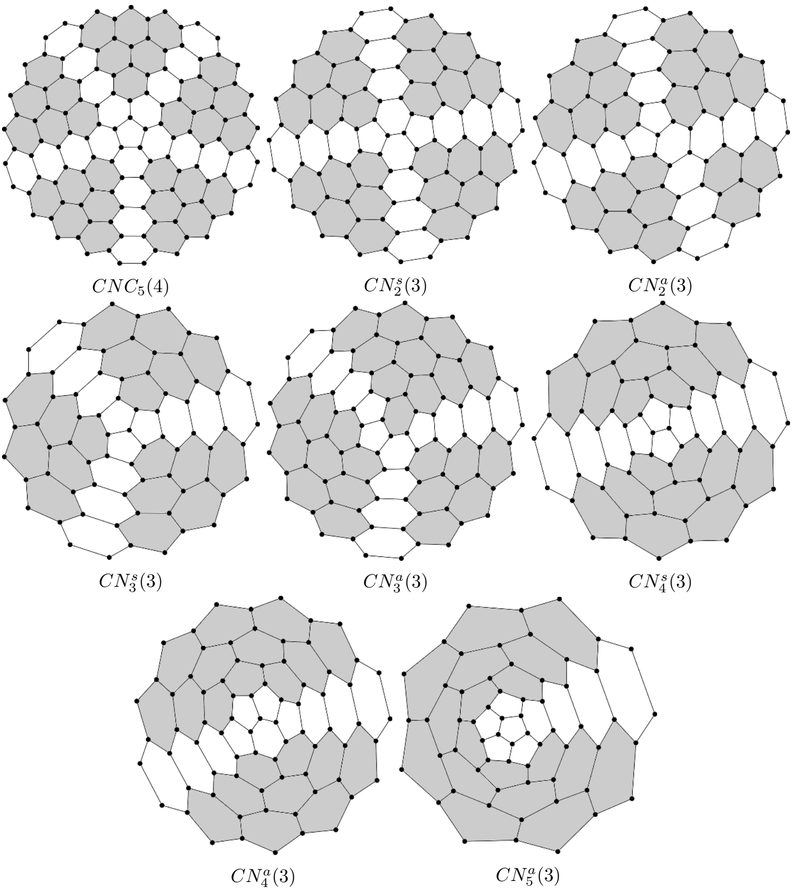

Figure 11. Nanocones split into benzenoid triangles, or subgraphs thereof, which are represented by the shaded regions.

Proof (of Theorem 2.6). Observe that a nanocone with s break edges can be split into s benzenoid triangles, or subgraphs of benzenoid triangles. Each such benzenoid triangle or subgraph resides between successive hexagons containing the break edges each layer of hexagons, see Figure 11. The sizes of the triangles depends on the lengths of the sides of the nanocone. Lemma 2.5 can be used to find a maximal matching of the benzenoid triangles of the indicated size. The union of these matchings augmented by a matching of size at most $s(\ell+1)$ along the break edges from each layer, and potentially an additional matching of the cap, gives an upper bound on the size of a maximal matching of the nanocone. Additional details for each case are provided below.

(a) $CNC_k(\ell)$ has k break edges and therefore can be split into k benzenoid triangles $T_{\ell-1}$, each triangle with a matching of size $\left\lfloor \frac{\ell(\ell+2)}{3} \right\rfloor$. The union of these matching augmented by a matching of size at most $k(\ell+1)$ along the break edges from each layer provides an upper bound for a maximal matching of $CNC_k(\ell)$.

(b) By Lemma 2.4, $CN_2^s(\ell)$ has 4 break edges and can be split into 4 benzenoid triangles, T_ℓ, each with a matching of size $\left\lfloor \frac{(\ell+1)(\ell+3)}{3} \right\rfloor$. Their union augmented by a matching along the break edges of size at most $4(\ell+1)$, plus an addition edge needed for the remaining edges on the cap, yields the desired upper bound.

(c) By Lemma 2.4, $CN_2^a(\ell)$ has 4 break edges and can be split into 3 T_ℓ's each with a matching of size $\left\lfloor \frac{(\ell+1)(\ell+3)}{3} \right\rfloor$ and an additional $T_{\ell-1}$ with a matching of size $\left\lfloor \frac{\ell(\ell+2)}{3} \right\rfloor$. The break edges require at most $4(\ell+1)$ edges after which the cap requires 1 additional edge.

(d) By Lemma 2.4, $CN_3^s(\ell)$ has 3 break edges and can be split into 3 T_ℓ's each with a matching of size $\left\lfloor \frac{(\ell+1)(\ell+3)}{3} \right\rfloor$. The break edges union the cap of the nanocone require at most an additional $3(\ell+1)+1$ edges.

(e) Again using Lemma 2.4, $CN_3^a(\ell)$ has 3 break edges and can be split into $T_{\ell+1}$, T_ℓ, and a subgraph of $T_{\ell+1}$, which in total require at most

$$2\left\lfloor \frac{(\ell+2)(\ell+4)}{3} \right\rfloor + \left\lfloor \frac{(\ell+1)(\ell+3)}{3} \right\rfloor$$

matched edges. The break edges need at most $3(\ell+1)$ edges and the cap requires at most 2 edges, proving the desired bound.

(f) Lemma 2.4 gives that $CN_4^s(\ell)$ has 2 break edges. So $CN_4^s(\ell)$ can be split into two pieces which turn out to be subgraphs of $T_{\ell+1}$, and each subgraph has a maximal matching of size at most $\left\lfloor \frac{(\ell+2)(\ell+4)}{3} \right\rfloor$. The union of these matchings augmented by a matching of the break edges of size at most $2(\ell+1)$ along with a matching of size 3 for the remaining edges of the cap provides the desired maximal matching.

(g) Similar to the case in (f), $CN_4^a(\ell)$ can be split into subgraphs of $T_{\ell+1}$ and $T_{\ell+2}$

requiring at most

$$\left\lfloor \frac{(\ell+3)(\ell+5)}{3} \right\rfloor + \left\lfloor \frac{(\ell+2)(\ell+4)}{3} \right\rfloor$$

matched edges. The break edges again require at most $2(\ell+1)$ matched edges, after which the cap needs at most 4 edges.

(h) By Lemma 2.4, $CN_5^a(\ell)$ has 1 break edge and contains a subgraph of $T_{\ell+4}$, which according to Lemma 2.5 has a maximal matching of size at most $\left\lfloor \frac{(\ell+5)(\ell+8)}{3} \right\rfloor$. The break edges require at most $(\ell+1)$ matched edges and the cap needing an additional 6 matched edges. ■

5 Proofs for nanotubes

Proof (of Corollary 2.8). It follows that $ZT(\ell, m)$ has $2m\ell + 2m$ total vertices and two external defects at the ends of the cylinder. The external defects each have m vertices of degree 2, for a total of $2m$ degree 2 vertices. Now Theorem 2.1 gives that

$$\begin{aligned} s(ZT(\ell, m)) &\geq \frac{2m\ell + 2m}{3} - \frac{2m}{6} \\ &= \frac{m(2\ell+1)}{3}. \end{aligned}$$

■

Acknowledgments: The author would like to thank the anonymous referees for their helpful comments and suggestions which significantly improved the exposition of this manuscript. This work was partially supported by a SPARC Graduate Research Grant from the Office of the Vice President for Research at the University of South Carolina. I am extremely grateful to Tomislav Došlić, whose mentoring and hosting during the Summer 2015 eventually led to the completion of this work. I would also like acknowledge the software CaGe [6] which helped draw Figures 1 and 11 in this paper, and I would like to thank Nico Van Cleemput, who helped export graphs from CaGe to use in my initial experimentation. I would like to thank Michael Santana for a helpful discussion concerning Theorem 2.1.

References

[1] OEIS Foundation Inc. (2018), The On-Line Encyclopedia of Integer Sequences, http://oeis.org.

[2] V. Andova, T. Došlić, M. Krne, B. Lužar, R. Škrekovski, On the diameter and some related invariants of fullerene graphs, *MATCH Commun. Math. Comput. Chem.* **68** (2012) 109–130.

[3] V. Andova, F. Kardoš, R. Škrekovski, Sandwiching saturation number of fullerene graphs, *MATCH Commun. Math. Comput. Chem.* **73** (2015) 501–518.

[4] J. Bornhoft, G. Brinkmann, J. Greinus, Pentagon-hexagon-patches with short boundaries, *Eur. J. Comb.* **24** (2003) 517–529.

[5] G. Brinkmann, N. V. Cleemput, Classification and generation of nanocones, *Discr. Appl. Math.* **159** (2011) 1528–1539.

[6] G. Brinkmann, O. D. Friedrichs, S. Lisken, A. Peeters, N. V. Cleemput, CaGe - a virtual environment for studying some special classes of plane graphs - an update, *MATCH Commun. Math. Comput. Chem.* **63** (2010) 533–552.

[7] S. Cyvin, I. Gutman, *Kekulé Structures in Benzenoid Hydrocarbons*, Springer, Berlin, 1988.

[8] T. Došlić, On lower bounds of the number of perfect matchings in fullerene graphs, *J. Math. Chem.* **24** (1998) 359–364.

[9] T. Došlić, Fullerene graphs with exponentially many perfect matchings, *J. Math. Chem.* **41** (2007) 183–192.

[10] T. Došlić, Saturation number of fullerene graphs, *J. Math. Chem.* **43** (2008) 647–657.

[11] T. Došlić, T. Short, Maximal matchings in polyspiro and benzenoid chains, arXiv:1511.00590.

[12] T. Došlić, N. Tratnik, P. Ž. Pleteršek, Saturation number of lattice animals, *Ars Math. Contemp.* **15** ((2018)) 191–204.

[13] T. Došlić, I. Zubac, Saturation number of benzenoid graphs, *MATCH Commun. Math. Comput. Chem.* **73** (2015) 491–500.

[14] T. Došlić, I. Zubac, Counting maximal matchings in linear polymers, *Ars Math. Contemp.* **11** (2016) 255–276.

[15] J. E. Graver, G. Graves, Fullerene patches I, *Ars Math. Contemp.* **3** (2010) 104–120.

[16] C. Graves, J. McLoud–Mann, Side lengths of pseudoconvex fullerene patches, *Ars Math. Contemp.* **5** (2012) 291–302.

[17] C. Graves, J. McLoud–Mann, K. S. Rovira, Extending patches to fullerenes, *Ars Math. Contemp.* **9** (2015) 209–222.

[18] C. Justus, *Boundaries of Triangle–Patches and the Expander Constant of Fullerenes*, Ph.D. thesis, Universität Bielefeld (2007).

[19] F. Kardoš, D. Král', J. Miškuf, J. S. Sereni, Fullerene graphs have exponentially many perfect matchings, *J. Math. Chem.* **46** (2009) 443–447.

[20] D. J. Klein, Topo–combinatoric categorization of quasi-local graphitic defects, *Phys. Chem. Chem. Phys.* **4** (2002) 2099–2110.

[21] D. J. Klein, A. T. Balaban, The eight classes of positive–curvature graphitic nanocones, *J. Chem. Inf. Model.* **46** (2006) 307–320.

[22] H. W. Kroto, J. R. Heath, S. C. O'Brien, R. F. Curl, R. E. Smalley, C60: Buckminsterfullerene, *Nature* **318** (1985) 162–163.

[23] L. Lovász, M. D. Plummer, *Matching Theory*, North–Holland, Amsterdam, 1986.

[24] N. Tratnik, P. Ž. Pleteršek, Saturation number of nanotubes, *Ars Math. Contemp.* **12** (2017) 337–350.

[25] M. Yannakakis, F. Gavril, Edge dominating sets in graphs, *SIAM J. Appl. Math.* **38** (1980) 364–372.

[26] H. Zhang, F. Zhang, New lower bounds on the number of perfect matchings of fullerene graphs, *J. Math. Chem.* **30** (2001) 343–347.